ISSN 0036-0295, Russian Metallurgy (Metally), Vol. 2021, No. 4, pp. 426–429. © Pleiades Publishing, Ltd., 2021.
Russian Text © The Author(s), 2020, published in Deformatsiya i Razrushenie Materialov, 2020, No. 8, pp. 16–20.

STRUCTURE AND PROPERTIES OF THE DEFORMED STATE

Structure of Differentially Hardened Rails after Severe Plastic Deformation

V. E. Kormyshev[a], V. E. Gromov[a, *], Yu. F. Ivanov[b], and A. M. Glezer[c, d]

[a] *Siberian State Industrial University, Novokuznetsk, 654007 Russia*
[b] *Institute of High-Current Electronics, Siberian Branch, Russian Academy of Sciences, Tomsk, 634055 Russia*
[c] *Bardin Central Research Institute for Ferrous Metallurgy, Moscow, 105005 Russia*
[d] *National University of Science and Technology MISiS, Moscow, 119049 Russia*
**e-mail: gromov@physics.sibsiu.ru*

Received March 26, 2020; revised April 23, 2020; accepted April 27, 2020

Abstract—The laws and mechanisms of structure and phase formation in the rails subjected to severe plastic deformation during long-term operation in a railway are revealed. A highly defective surface layer ≈200 μm thick with a grain–subgrain nanostructure is found to form in the rails as a result of long-term operation. The mechanisms of transformation of cementite lamellae are discussed. The dissolution of cementite lamellae is shown to be accompanied by strain aging, which causes the formation of cementite nanoparticles (5–15 nm) in the ferrite lamellae volume.

Keywords: lamellar pearlite, long-term operation, nanocrystalline structure, formation mechanism
DOI: 10.1134/S0036029521040169

NTRODUCTION

The increasing speeds of railway trains and the contact pressures (more than 1 GPa) in the wheel–rail system are responsible for the processes (recrystallization, relaxation, phase transitions, amorphization) proceeding in the rail surface even after relatively small carried tonnage (100–500 mln t gross). These processes lead to the evolution of structural and phase states and corresponding degradation of the mechanical properties [1–7]. A so-called 100-μm-thick white layer forms due to long-term mechanical treatment at relatively low temperatures. The microstructure of this layer is extremely heterogeneous, the grain size distribution is bimodal, and the grain sizes change in the range from 20 to 500 nm [1, 2].

The formation of nanograins in pearlitic steels under contact loading in the wheel–rail system was shown to be a multistage process [3]. At the first stage, pearlite as a whole undergoes plastic deformation, the distance between lamellae decreases, a large number of dislocations forms in ferrite, the thickness of the cementite plates decreases, and some of them fail and dissolve. Ferrite grain refinement stops when their sizes reach a stable minimum value. Cementite continues to dissolve due to dislocation accumulation. Its dissolution stops when the rate of accumulation and the rate of annihilation of dislocations reach equilibrium. Refinement of ferrite grains to 10 nm in pearlitic steel (0.86% C) during severe plastic deformation by high-pressure torsion is accompanied by complete dissolution of cementite [4], which also proceeds in several stages. Thus, the behavior of rail steel during long-term operation is very close to the behavior of metallic materials during severe deformation [5, 6].

We should note that, despite the difference in the deformation techniques (equal-channel angular pressing [7–9], high pressure torsion in the Bridgman camera [10], multidirectional isothermal forging [11]) used to achieve megaplastic deformation, pearlitic steel under external loading behaves like a two-phase heterogeneous medium. The basic mechanisms of structure formation and evolution in pearlitic steel during megaplastic deformation are the formation of ferrite nanograins, the deformation-induced refinement of cementite lamellae due to shear stresses, and the subsequent formation of nanosized cementite at dislocations and at ferrite nanograin boundaries due to the migration of carbon atoms mainly along dislocation cores.

The manyfold differential hardening of 100-m rails after the passage of a tonnage of 691.8 mln t gross was analyzed in [12–15]. The specific features of hardening by carbide phase particles, hardening caused by pearlitic structure formation and dislocation substructure formation, hardening by long-range stress fields, and precipitation hardening were considered. This work was aimed at finding the laws and mechanisms of structural and phase formation in the railhead fillet after long-term operation in a railway.

Table 1. Element contents in the DT350 rail (wt %)

Parameter	C	Mn	Si	P	S	Cr	Ni	Cu	V	Al	Ti
Sample	0.72	0.77	0.61	0.010	0.009	0.42	0.07	0.14	0.038	0.003	0.003
Requirements*	0.71–0.82	0.75–1.25	0.25–0.60	No more than		0.20–0.80	No more than 0.27 in total		0.03–0.15	No more than	
				0.020	0.020		0.20	0.20		0.004	0.025

* Requirements of TU 0921-276-01124323–2012 for E76KhF steel.

EXPERIMENTAL

100-m DT350 rails subjected to differential hardening during the passage of a tonnage of 1411 mln t gross were studied. The chemical composition of the rail sample metal met the requirements of TU 0921-276-01124323–2012 for E76KhF steel (Table 1).

The structure was examined by optical (Olympus GX51), scanning (TESCAN MIRA 3), and transmission electron (EM-125) microscopy. The macrostructure was estimated in accordance with RD 14-2R-5–2004 Classifier of Macrostructure Defects in Rails Rolled from Continuous Cast Electric Furnace Steel Billets. The microstructure was studied on polished sections taken at the top of the railhead fillet and at a distance of 0.5–1.0 mm from it. Foils 150–200 nm thick for transmission electron microscopy (TEM) were prepared by electrolytic thinning of plates spark-cut at the surface and at a distance of 2 and 10 mm from it (Fig. 1).

RESULTS AND DISCUSSION

The main structural constituent of the steel are lamellar grains of highly dispersed pearlite. A quantitative analysis of the steel microstructure revealed the following: the grain size was 15.04–51.17 μm (average size was 29.8 μm), the size of pearlite colonies was 2.71–12.16 μm (average size was 6.17 μm), and the interlamellar distance was 73–256 nm (average was 132 nm). Figure 2 shows the histograms of the distribution of the interlamellar distances and the lamellar pearlite colony sizes.

The amount of degenerated pearlite colonies with globular cementite in them and structurally free ferrite grains in the structure is significantly lower. A dislocation substructure exists in the volume of these grains and the ferritic constituent of the pearlite colonies. Dislocations are distributed predominantly chaotically. They form dislocation pileups less frequently. Cementite lamellae in pearlitic colonies are also defective. The contrast in the volume of these lamellae indicates the formation of misoriented regions (fragments) in them.

The metal of the rails is in an elastically strained state. This fact is indicated by lattice bending and torsion accompanied by the appearance of bended extinction contours in electron-microscopic images [1, 16, 17], which was observed during structural examination of steel foils by TEM (Fig. 3). As a rule,

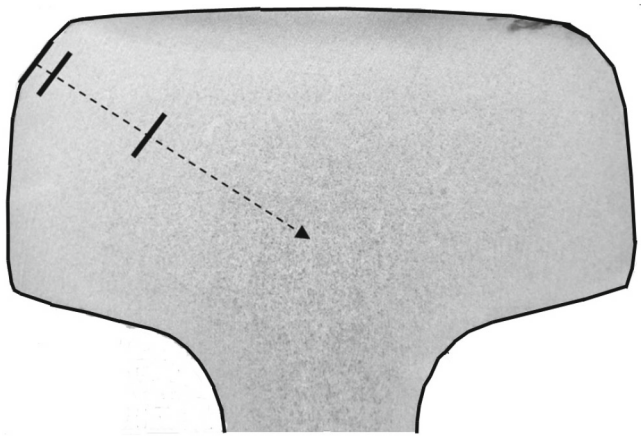

Fig. 1. Transverse template of the rail head. The sites of taking samples for foil preparation are indicated.

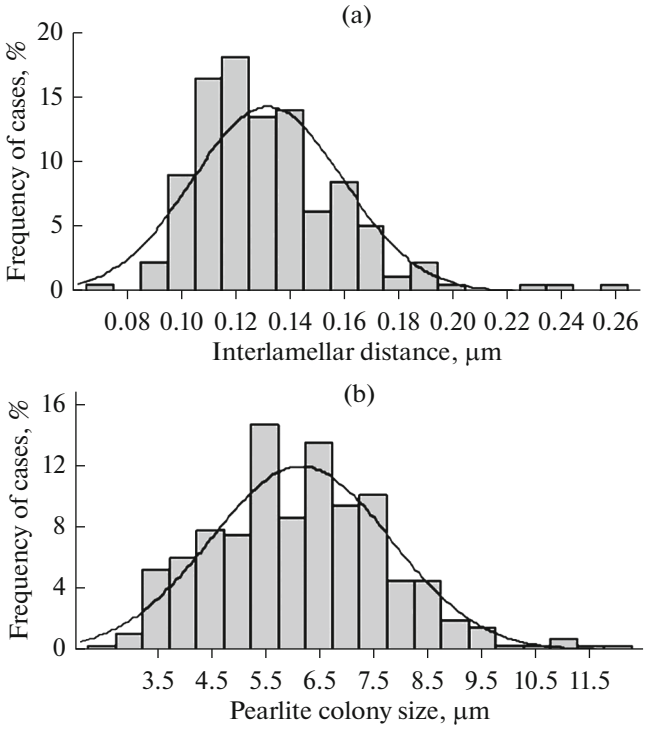

Fig. 2. (a) Interlamellar distance and (b) pearlite colony size distributions at a distance of 0.5–1.0 mm from the rail surface.

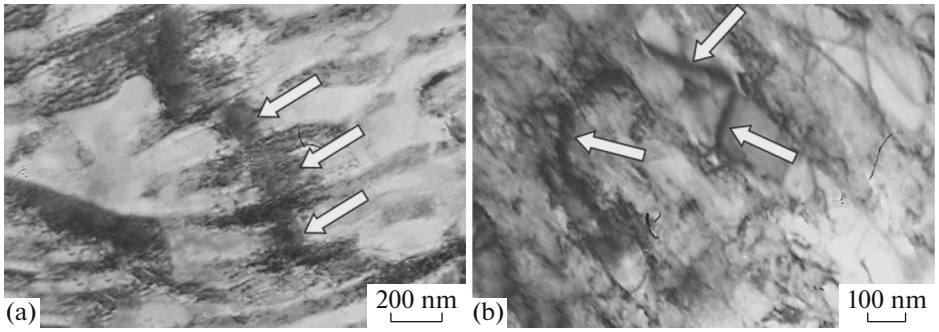

Fig. 3. Electron-microscopic image of the structure of lamellar pearlite (layer at a depth of 2 mm): (a) pearlite colony and (b) ferrite lamellae. The arrows indicate bend extinction contours.

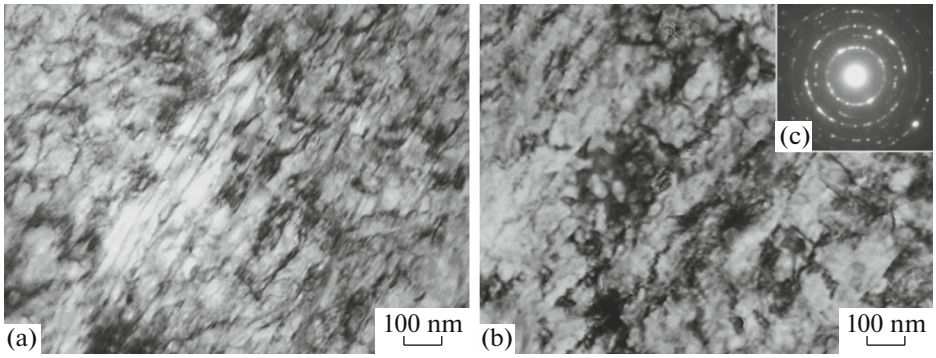

Fig. 4. Electron-microscopic image of the pearlite structure of the surface layer of the railhead fillet: (a) pearlite colony, (b) grain–subgrain structure of pearlite colonies, and (c) electron diffraction pattern to (b).

contours intersect a pearlite colony, passing from one ferrite lamella to the other, which indicates bending and torsion of the colony as a whole (see Fig. 3a). A bend contour is located within a single ferrite lamella very rarely, which demonstrates bending and torsion of the crystal lattice of the lamella (see Fig. 3b).

The surface layer ≈200 μm thick in the rail fillet zone has a significantly different structure. This layer contains many defects due to heat and mechanical treatment during long-term operation of the rails. TEM showed that long-term operation resulted in the formation of a grain–subgrain structure with crystallites 40–50 nm in size in the pearlite colonies (Fig. 4). The ring-like electron diffraction patterns point to nanostructuring of the pearlite colonies (see Fig. 4c). Fracture of cementite lamellae is also observed. There are two mechanisms of their fracture: (i) cutting of cementite lamellae by moving dislocations followed by motion of their fragments and (ii) dissolution due to the motion of carbon atoms from the cementite lattice to the dislocations surrounding a lamella. This process is completed by the formation of nanosized (5–15 nm) round-shaped cementite particles in the ferrite lamellae volume (Fig. 5), which indicates aging. Structur-

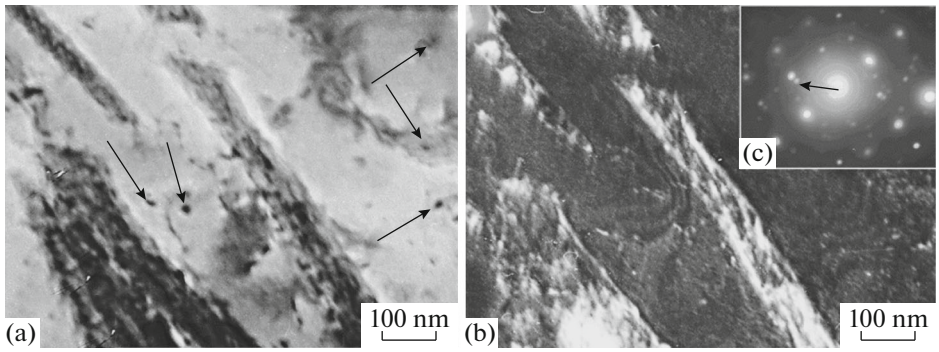

Fig. 5. (a) Bright-field and (b) dark-field images of cementite lamellae undergoing fracture by the dissolution mechanism. (c) Electron diffraction pattern to (a). The arrow indicates the [110] α-Fe and [201] Fe_3C reflections, which were used to take the dark-field image in (b). The arrows in (a) indicate globular cementite particles located in ferrite lamellae.

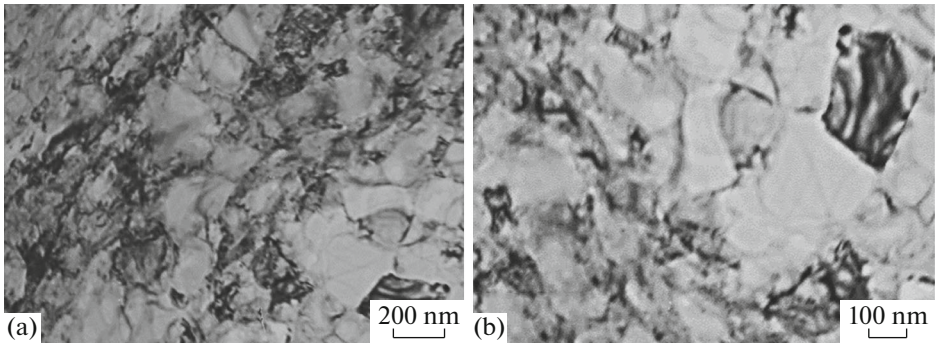

Fig. 6. Electron-microscopic image of the structure of the surface layer in the railhead fillet.

ally-free ferrite grains were also fragmented (Fig. 6a). The fragments practically are free of dislocations, and the fragment size is 150–250 nm (Fig. 6b).

CONCLUSIONS

Our experimental results revealed severe (megaplastic) deformation in a ≈200-μm-thick surface layer in rails, which causes a significant transformation of lamellar pearlite and the formation of submicro- and nanocrystalline structures.

FUNDING

This work was supported by the Russian Foundation for Basic Research, project no. 19-32-60001.

REFERENCES

1. V. E. Gromov, O. A. Peregudov, Y. F. Ivanov, et al., *Evolution of Structure-Phase States of Rail Metal in Long-term Operation* (Izd. SO RAN, Novosibirsk, 2017).
2. Yu. Ivanisenko and H. J. Fecht, "Microstructure modification in the surface layers of railway rails and wheels: effect of high strain rate deformation," Steel Tech. **3** (1), 19–23 (2008).
3. R. Pan, R. Ren, C. Chen, and X. Zhao, "Formation of nanocrystalline structure in pearlitic steels by dry sliding wear," Mater. Charact., **132**, 397–404 (2017).
4. Yu. Ivanisenko, W. Lojkowski, R. Z. Valiev, and H.-J. Fecht, "The mechanism of formation of nanostructure and dissolution of cementite in a pearlitic steel during high-pressure torsion," Acta Mater. **51** (18), 5555–5570 (2003).
5. Yu. F. Ivanov, V. E. Gromov, A. M. Glezer, O. A. Peregudov, and K. V. Morozov, "Nature of the structural degradation of rail surfaces during operation," Bull. Russ. Acad. Sci.: Phys. **80** (12), 1682–1687 (2016).
6. A. M. Glezer, "On the nature of ultrahigh plastic (megaplastic) deformation," Izv. Ross. Akad. Nauk, Ser. Fiz. **71** (12), 1767–1776 (2007).
7. R. Z. Valiev and I. V. Aleksandrov, *Bulk Nanostructured Materials: Synthesis, Structure, and Properties* (Nauka, Moscow, 2007).
8. R. A. Andrievskii, *Foundations of Nanostructure Materials Science. Opportunities and Problems* (Binom. Lab. Znanii, Moscow, 2012).
9. A. Vinogradov and Yu. Estrin, "Analytical and numerical approaches to modeling severe plastic deformation," Prog. Mater. Sci. **95**, 172–242 (2018).
10. A. M. Glezer, "Principles of creating multifunctional structural materials of new generation," Usp. Fiz. Nauk **182** (5), 559–566 (2012).
11. Z. Gronostajski, Z. Pater, L. Madej, and P. Surdacki, "Recent development trends in metal forming," Arch. Civ. Mech. Eng. **19** (3), 898–941 (2019).
12. V. E. Gromov, A. A. Yuriev, O. A. Peregudov, S. V. Konovalov, Yu. F. Ivanov, A. M. Glezer, and A. P. Semin, "Physical nature of structure and properties degradation of rail surface after long term operation," AIP Conf. Proc. **1909**, 020066 (2017).
13. V. E. Gromov, A. A. Yuriev, Yu. F. Ivanov, A. M. Glezer, S. V. Konovalov, A. P. Semin, and R. V. Sundeev, "Defect substructure change in 100-m differentially hardened rails in long-term operation," Mater. Lett., **209**, 224–227 (2017).
14. A. A. Yur'ev, V. E. Gromov, K. V. Morozov, and O. A. Peregudov, "Long-term surface changes in differentially quenched 100-m rail," Steel Transl. **47**, 658–661 (2017).
15. Yu. F. Ivanov, V. E. Gromov, A. A. Yur'ev, A. M. Glezer, N. A. Popova, O. A. Peregudov, and S. V. Konovalov, "Contributions of various mechanisms to the hardening of differentially quenched rails during long-term operation," Rus. Metall. (Metally), No. 10, 789–794 (2018).
16. P. Hirsch, A. Howie, P. Nicholson, et al., *Electron Microscopy of Thin Crystals* (Mir, Moscow, 1968).
17. A. N. Tyumentsev, A. D. Korotaev, I. A. Ditenberg, Yu. P. Pinzhin, and V. M. Chernov, *Laws of Plastic Deformation in High-Strength and Nanocrystalline Metallic Materials* (Izd. SO RAN, Novosibirsk, 2018).

Translated by T. Gapontseva